Two Distinct Regulatory Systems Control Pulcherrimin Biosynthesis in *Bacillus subtilis*

Nicolas L. Fernandez[1] and Lyle A. Simmons[1*]

[1]Department of Molecular, Cellular, and Developmental Biology, University of Michigan, Ann Arbor, MI 48109

*LAS: Department of Molecular, Cellular, and Developmental Biology, University of Michigan, Ann Arbor, Michigan 48109-1055, United States. Phone: (734) 763-7142, Fax: (734) 647-0884 E-mail: lasimm@umich.edu

Short title: Transcriptional Regulation of Pulcherrimin Biosynthesis

Keywords: transcription factor, pulcherrimin, *Bacillus subtilis,* transition state

Abstract

Regulation of transcription is a fundamental process that allows bacteria to respond to external stimuli with appropriate timing and magnitude of response. In the soil bacterium *Bacillus subtilis,* transcriptional regulation is at the core of developmental processes needed for cell survival. Gene expression in cells transitioning from exponential phase to stationary phase is under the control of a group of transcription factors called transition state regulators (TSRs). TSRs influence numerous developmental processes including the decision between biofilm formation and motility, genetic competence, and sporulation, but the extent to which TSRs influence bacterial physiology remains to be fully elucidated. Here, we demonstrate two TSRs, ScoC and AbrB, along with the MerR-family transcription factor PchR negatively regulate production of the iron chelator pulcherrimin in *B. subtilis.* Genetic analysis of the relationship between the three transcription factors indicate that all are necessary to limit pulcherrimin production during exponential phase and influence the rate and total amount of pulcherrimin produced. Similarly, expression of the pulcherrimin biosynthesis gene *yvmC* was found to be under control of ScoC, AbrB, and PchR and correlated with the amount of pulcherrimin produced by each background. Lastly, our in vitro data indicate a weak direct role for ScoC in controlling pulcherrimin production along with AbrB and PchR. The layered regulation by two distinct regulatory systems underscores the important, and somewhat enigmatic, role for pulcherrimin in *B. subtilis* physiology.

Author Summary

Regulation of gene expression is important for survival in ever changing environments. In the soil bacterium *Bacillus subtilis,* key developmental processes are controlled by overlapping networks of transcription factors, some of which are termed transition state regulators (TSRs). Despite decades of research, the scope of how TSRs influence *B. subtilis* physiology is still being uncovered. We found that three transcription factors, two of which are TSRs, converge to inhibit production of the iron-chelator pulcherrimin. Only when all three are missing is pulcherrimin production elevated. Finally, we demonstrate that expression of pulcherrimin biosynthesis genes occurs via direct and indirect regulation by the trio of transcription factors. Due to its iron chelating ability, pulcherrimin has been characterized as a modulator of niche development with antioxidant properties. Thus, our findings that TSRs control pulcherrimin, concurrently with other developmental phenotypes, provides new insight into how TSRs impact *B. subtilis* and its interaction with the environment.

Introduction

In the soil bacterium *Bacillus subtilis,* complex arrays of gene networks function together to precisely time the expression of gene products. A prime example is the series of decisions made as cells transition from exponential growth to stationary phase upon nutrient limitation [1]. This phase, termed the transition state, is where cells in the population use environmental cues to inform the next course of action to survive in the new environment, specifically whether to engage in competence, biofilm formation, motility, secondary metabolism, and/or acquisition of nutrients [1]. While there are many transcription factors controlling these processes, an important set among these are called transition state regulators (TSRs).

Originally defined in the context of sporulation, TSRs are regulators that inhibit expression of genes involved in developmental processes but do not result in a sporulation null mutation when deleted [2,3]. Notably, mutants in TSRs are still able to carry out post-exponential phenotypes, however the magnitude and timing of these phenotypes are disrupted [4]. ScoC and AbrB represent two well-studied TSRs in *B. subtilis.* ScoC is a MarR-family winged helix-turn-helix transcription factor first identified in hyper-protease mutants [5,6]. Microarray analysis between WT and *scoC* mutants identified 560 genes with differential gene expression involved in motility and genetic competence as well as protease production and peptide transport [7]. The smaller AbrB (10.8 kDa) is part of a large family of transcription factors with a beta-alpha-beta DNA binding N-terminal domain [8]. Mutants of *abrB,* like *scoC,* have pleiotropic effects with some overlap with ScoC [9,10]. ChiP-seq analyses of AbrB identified many binding sites with a bipartite TGGNA motif [11].

Pulcherrimin is a secreted iron chelating molecule that has been a topic of research in *Bacillus subtilis* and other microorganisms [12–16]. Pulcherrimin is synthesized by the 1) cyclization of two tRNA-charged leucines to form cyclo-L(leucine-leucine) (cLL) and 2) oxidation to form water-soluble pulcherriminic acid **(Fig. 6A).** Pulcherriminic acid is then transported outside of the cell where it can bind to free ferric iron to form the water-insoluble pulcherrimin **(Fig. 6A).** Past work has demonstrated that pulcherrimin biosynthesis is under control of the MarR-family transcription factor PchR, which is found adjacent to genes involved in pulcherrimin biosynthesis and transport in *B. subtilis* [12,13]. Interestingly, an AbrB binding site has been identified in the promoter for pulcherrimin biosynthesis genes, suggesting AbrB was involved in pulcherrimin biosynthesis [9,11]. Whether other TSRs were involved in regulation pulcherrimin production is not known.

In this study, we provide evidence of multi-layered regulation of pulcherrimin biosynthesis by the TSRs ScoC and AbrB as well as the pulcherrimin regulator PchR. We explore the kinetics of pulcherrimin production throughout the transition state and found that ScoC, AbrB, and PchR control the timing, rate, and amount of pulcherrimin produced by modulating expression of the pulcherrimin biosynthetic gene cluster *yvmC-cypX.* We further establish the roles of PchR and AbrB in direct regulation of gene expression utilizing in vitro DNA binding assays and provide evidence that ScoC can bind directly to the *yvmC* promoter in vitro. Together our results suggest a model where pulcherrimin biosynthesis is regulated by nutrient levels during the transition from exponential phase to stationary phase in addition to input from PchR, linking stationary phase with extracellular iron sequestration.

Methods

Bacterial Strains and Culturing

A derivative of the wild-type strain 3610 *Bacillus subtilis* harboring an amino acid substitution in the competence inhibitor ComI (Q12I) was used as the background strain in these studies [17]. Gene replacements and deletions were constructed as described [18]. Gel purified gene-targeting antibiotic resistance cassettes and non-replicative plasmids (see Cloning for construction details) were used to transform *B. subtilis* by natural transformation. Briefly, single colonies of the strain of interest were inoculated into 1 mL LB supplemented with 3 mM $MgSO_4$ and grown to mid-log phase while shaking at 230 RPM at 37°C. The cultures were then back diluted 1:50 into 2 mL MD media (1X PC buffer [10X PC - 10.7 g K_2HPO_4, 6 g KH_2PO_4, 1.18 g trisodium citrate dehydrate, deionized water to 100 ml, filter sterilize], 2% glucose, 0.05 mg/mL tryptophan, 0.05 mg/mL phenylalanine, 0.01 mg/mL ferric ammonium citrate, 2.5 mg/ml potassium aspartate, 3 mM $MgSO_4$, water up to 2 mL) and grown for 3-5 hours, until early stationary phase. 10 µL of purified gene-targeting antibiotic resistance cassettes (~200-400 ng total) were added to 0.2 mL competent *B. subtilis,* were further incubated one hour, and plated on LB agar plate supplemented with either erythromycin (50 µg/mL), kanamycin (10 µg/mL), chloramphenicol (5 µg/mL), and/or spectinomycin (100 µg/mL). Antibiotic resistance clones were restruck on selection and insertions were verified by colony PCR using the US forward and DS reverse primers (See S Table 1). To remove the antibiotic resistance cassette, plasmid pDR224 was used to transform the appropriate strain with transformants selected for on LB supplemented with spectinomycin (100 µg/mL). Spectinomycin resistant clones were struck out on LB and incubated at the non-

permissive temperature of 42ºC; this process was repeated twice. Clones were then rescreened for sensitivity of spectinomycin and the absence of the integrated antibiotic resistance cassette using PCR.

Cloning

To generate gene disruptions, oligos were designed to amplify upstream (US) and downstream (DS) of the gene of interest with appropriate overhangs to fuse either an erythromycin or kanamycin resistance cassette (AbR) flanked by CRE recombinase recognition sites [18]. Oligonucleotides were designed using NEBuilder (NEB) with the default parameters except minimum overlap length was changed from 20 nucleotides to 30 nucleotides. Q5 polymerase (NEB) was used to amplify the appropriate PCR amplicon. All amplicons were gel extracted prior to assembly reactions (Qiagen). US, DS, and AbR fragments were assembled by splice by overlap extension (SOE) PCR (adapted from [19]). First, 0.5 pmol each of the US, DS, and AbrB amplicons were mixed with 18 µL Q5 5X buffer, 0.25 mM dNTPs, and water up to 89 µL. 1 µL Q5 (2U) was added, and PCR was carried out with the following parameters: 1 cycle of 98°C – 10s, 10 cycles of 98°C – 10s, 55°C – 30s, 72°C – 2 minutes, 1 cycle of 72°C – 10 minutes. After completion of the PCR, 5 µL of US forward prime and 5 µL of the DS reverse primer were added and PCR was set under the following conditions: 1 cycle of 98°C – 2 minutes, 15 cycles of 98°C – 10s, 55°C – 30s, 72°C – 3 minutes, 1 cycle of 72°C – 10 minutes. Following PCR, spliced amplicons were analyzed on a gel and 10 µL used directly for transformation into competent *B. subtilis.*

Vectors for protein purification (pNF039, pNF040, and pTMN007) and homologous recombination (pNF038) in *B. subtilis* were constructed using Gibson Assembly (NEB)

following the manufacturer's protocol. Protein expression vectors were used to transform *E. coli* DH5alpha and homologous recombination vectors were used to transform *E. coli* MC1061 and clones were verified via sanger sequencing (Azenta) or whole plasmid sequencing (Eurofins). All primers and assembly methods are included in S Table 1. To generate a *pyvmC*-GFP transcriptional fusion (pNF047), plasmid pYFP-STAR was amplified with the primer pair oNLF554-oNLF555 and gel extracted. The ORF for sfGFP was amplified from plasmid pDR110-GFP(Sp) using the primer pair oLVG035A-oLVG035B and gel extracted. The *pyvmC* locus was amplified in two fragments: 1) oNLF524-525 and 2) oNLF526-527. The resulting fragments were then assembled by Gibson Assembly (NEB), transformed into MC1061 *E. coli* cells by heat shock, and transformants were selected for by plating on LB Amp plates. The assembled plasmid consisted of the *pyvmC* promoter lacking 17 nucleotides upstream of the ATG start codon of *yvmC,* deleting the native ribosome binding site which can contribute to spurious translation and high GFP background [20].

Media

WT and derived *B. subtilis* strains were either grown in Luria broth or Tris-Spizizen salts (TSS) [Reagents added in order: 50 mM Tris pH 7.5, 136 µM trisodium citrate dihydrate, water up to final volume, 2.5 mM dibasic potassium phosphate, 811 µM $MgSO_4$, 1X $FeCl_3$ from a 100X stock solution [150 µM $FeCl_3$, 0.1 g trisodium citrate dihydrate, 100 mL deionized water, filter sterilized], 0.5% glucose [25% stock solution, filter sterilized], and 0.2% ammonium chloride [20% stock solution, filter sterilized]. For liquid TSS, all components were mixed, filter sterilized, stored in the dark, and used within a week. For TSS agar plates, all reagents, except the 1X $FeCl_3$ solution, glucose, and ammonium

chloride, were mixed with agar at 1.5% w/v and autoclaved. After the agar solution cooled to approximately 55°C, filter sterilized $FeCl_3$, glucose, and ammonium chloride were added, approximately 20-25 mL were added to sterile petri plates, and plates were allowed to dry overnight. TSS agar plates were stored at 4°C and were used within 6 months.

Spot plating and liquid culture imaging

One day prior to the spotting, TSS plates with varying concentrations of $FeCl_3$ (final concentrations: 0.15, 1.5, 15, and 150 μM $FeCl_3$) were poured and dried overnight at room temperature. Spots for Fig. 1 were on TSS plates supplemented with 150 μM $FeCl_3$. Strains were inoculated from frozen stocks into 1 mL TSS media and grown overnight at 37°C while shaking at 250 RPM. The next day, the turbidity of each culture was measured and adjusted to an OD_{600} of 1.0 in fresh TSS media. 10 μL of each culture were spotted 15 mm apart on the same TSS plate and incubated for 24hr at 30°C. The next day, plates were imaged using an imaging box [21] and an iPhone 7 running iOS 15.7.5. Images were cropped and arranged using Adobe Photoshop and Illustrator. Each experiment included two technical spotting replicates and was repeated at least twice on separate days. For liquid cultures, 2 mL overnights were started from frozen stocks in TSS media and grown overnight at 37°C while shaking at 250 RPM. Overnight cultures were diluted to a starting OD_{600} of 0.05 in 40 mL TSS in 125 mL flasks and grown for 20-24 hours at 37°C while shaking at 250 RPM. Images of the flasks were taken as stated above.

LC/MS for cyclo-dileucine measurement

WT and *yvmC::erm* were struck out onto TSS plates from frozen stocks and grown overnight at 37°C for 16 hours. The next day, the strains were washed from the plate into fresh TSS and the resulting culture was used to inoculate 16 mL TSS in 50 mL flask at a starting OD_{600} of 0.050. Cultures were grown for 6 hours while shaking at 250 RPM at 37°C. After six hours (OD_{600} ~ 1.0), 15 mL of culture was collected by centrifugation in a 15-mL falcon tube (3 minutes, 4200xg) and the resulting pellets were resuspended in 200 µL cold extraction buffer (acetonitrile:methanol:water, 40:40:20, [22]). The resulting cellular mixture was centrifuged in a microcentrifuge (30s, 15,000 x g) and the supernatant containing the extracted metabolites were moved to a new 1.5 mL microcentrifuge tube and frozen at -80C. Samples were sent to the Michigan State University Research Technology Support Facility for LC-MS analysis of cyclo-dileucine. Two hundred microliter of the extract was evaporated to dryness using a SpeedVac and resuspended with an equal volume of methanol: water, 1:9 (v/v). Ten microliter of the sample was injected onto an Acquity Premier HSS T3 column (1.8 µm, 2.1 x 100 mm, Waters, Milford, MA) and separated using a 10 min gradient as follows: 0 to 1 min were 100% mobile phase A (0.1% formic acid in water) and 0% mobile phase B (acetonitrile); linear ramp to 99% B at 6 min, hold at 99% B until 8 min, return to 0% B at 8.01 min and hold at 0% B until 10 min. The column was held at 40°C and the flow rate was 0.3 mL/min. The mass spectrometer (Xevo G2-XS QToF, Waters, Milford, MA) was equipped with an electrospray ionization source and operated in positive-ion and sensitivity mode. Source parameters were as follows: capillary voltage 3000 V, cone voltage 30V, desolvation temperature 350 °C, source temperature 100 °C, cone gas flow 40 L/hr, and desolvation

gas flow 600 L/Hr. Mass spectrum acquisition was performed in positive ion mode with a range of m/z 50 to 1500 with the target enhancement option tuned for m/z 227. A calibration curve was made using cyclo-dileucine standard (Santa Cruz Biotechnology). The peak area for cyclo-dileucine was integrated based on the extracted ion chromatogram of m/z 227.18 with an absolute window of 0.05 Da. Peak processing was performed using the Targetlynx tool in the Waters Masslynx software.

Pulcherrimin Isolation and Measurement

Strains of interest were struck out on TSS agar plates from frozen stocks and incubated overnight (16-20 hours) at 37°C. The next day, cells were collected by adding 1 mL fresh TSS media to the plates and gently swirling to remove bacteria adhered to the agar. The resulting bacterial suspension was then moved to microcentrifuge tubes, the OD_{600} recorded, and diluted to a starting OD_{600} of 0.05 in 40 mL TSS media in 125 mL round bottom flasks. At the time indicated, 1.5 mL of culture was aliquoted into a microcentrifuge tube. 0.1 mL were used for OD_{600} measurement while the remaining cells were collected by centrifugation (10,000 x g, 30s). The supernatant was removed and the cell pellet and insoluble pulcherrimin were resuspended in 0.1 mL 2M NaOH by pipetting the solution until completely resuspended. The samples were then centrifuged again (10,000 x g, 1 minute) and the supernatant were moved to clean wells in a 96-well plate and absorbance at 410 nm was measured using a Tecan M200 plate reader.

To determine the time of entry into stationary phase, the R package growthrates was used to fit a linear growth model for every strain and replicate [23]. The time in which the growth data deviated from exponential growth was used as time 0 for Fig. 2. The grow_gompertz3 function was used to model the change in absorbance at 410 nm over

time using the growthrates package [23]. Each strain and replicate (n = 3) were modeled individually and the resulting parameters (maximum growth rate [mumax] and carrying capacity (abs. 410 nm) [K]) were summarized by taking the average and standard deviation plotted in Fig. 1B. For the production start time, curves were analyzed manually to determine when the predicted A_{410} from the mutant strain deviated from the predicted A_{410} value from the WT background during exponential phase. For duration of pulcherrimin production, the x-axis distance between the beginning of the exponential phase of pulcherrimin production and the start of the stationary phase of pulcherrimin production were measured manually.

Epistasis Analysis

Epistasis of double mutants were determined by applying the multiplicative model of epistasis, which states a series of gene deletions are epistatic if the sums of the single mutant phenotype (expected) are different than the phenotype of the double mutant (observed) [24]. Values greater than zero indicate positive epistasis while values less than zero indicate negative epistasis.

Fluorescence Reporter Assay

WT and isogenic mutants harboring the *pyvmC*-GFP transcriptional fusion at the *amyE* loci were struck out on TSS agar plates and grown overnight for ~ 16 hours at 37°C. The next day, the strains were plate washed into 1 mL TSS media and the OD_{600} was recorded. 40 mL TSS in 125 mL Erlenmeyer flasks were inoculated with the plate washed cells at a starting OD_{600} of 0.050. The cultures were incubated at 37°C while shaking at 250 RPM until the cultures reached mid-exponential phase. Fluorescence was measured

from a 1 mL sample using an Attune NxT Acoustic Focusing Cytometer (ThermoFisher Scientific) using the following settings: Flow rate, 25 µl/min; FSC voltage, 200; SSC voltage, 250; BL1 voltage, 250 [25].

Protein Purification

ScoC purification was carried out as previously described with some minor amendments [25]. Plasmid pTMN007 harboring ScoC in a T7 expression vector pE-SUMO was use to transform BL21-DE3 *E. coli* and plated on LB supplemented with kanamycin (25 µg/mL). The next day, a single colony was inoculated into 1 mL LB Kan_{25}, grown to mid-exponential phase at 37°C while shaking at 230 RPM, diluted 1:5 in 5 mL LB Kan_{25}, and grown overnight at 37°C while shaking at 37°C. After overnight growth, the culture was diluted to a starting OD_{600} of 0.05 in 400 mL LB Kan_{25} at 37°C shaking at 230 RPM and grown until the OD_{600} reached between 0.7, after which 1 mM final concentration of Isopropyl ß-D-1-thiogalactopyranoside (IPTG) was added to induce protein expression for three hours at 37°C. After induction, cells were collected by centrifugation (5 minutes at 7,500 RPM using SLA-1500 rotor in a Sorvall RC 5B plus centrifuge) and cell pellets were stored at -20C until use. Cell pellets were thawed at room temperature and resuspended in 40 mL lysis buffer (50 mM Tris pH 8, 300 mM NaCl, 10% sucrose, 10 mM imidazole, and 1 EDTA-free protease inhibitor tablet added the day of purification (Roche)). The cell solution was moved to a beaker in an ice-water bath and was sonicated (15s ON, 25s OFF, 24 cycles, 50% amplitude, Fisher Scientific Model 505 Sonic Dismembrator). The lysate was cleared by centrifugation (10 minutes, 12,000 RPM, using an SS-34 rotor in a Sorvall RC 5B plus centrifuge). The clarified lysate was loaded onto a 3 mL Ni-NTA column pre-equilibrated with lysis buffer and the flow through was

discarded. The column was washed three times with 20 mL wash buffer (50 mM Tris pH 8, 2M NaCl, 25 mM imidazole, and 5% glycerol) and ScoC-SUMO-His was eluted with 15 mL elution buffer (50 mM Tris pH 8, 150 mM NaCl, 200 mM imidazole). The protein solution was dialyzed at 4°C into dialysis buffer (50 mM Tris pH 8, 150 mM NaCl, 5% glycerol). The next day, DTT (1 mM) and SUMO Ulp1 protease were added, the solution was incubated at room temperature for 2 hours and dialyzed into dialysis buffer overnight at 4°C. Following dialysis, SUMO-free ScoC was purified by loading the solution onto 3 mL of pre-equilibrated Ni-NTA resin by collecting the flow through. SUMO-free ScoC fractions were determined via SDS-PAGE, pooled, quantified by the Bradford assay, diluted with glycerol for a final concentration of 25%, and stored at -80°C.

Expression vectors for PchR and AbrB were constructed similar to ScoC. Growth of BL21 *E. coli* harboring PchR was identical to ScoC. Growth of BL21 *E. coli* harboring AbrB had the following changes. First, 1 mL LB Kan was inoculated with a single colony of *E. coli* harboring the AbrB expression vector and grown for 6 hours at 37°C, shaking at 200 RPM. The 1 mL culture was diluted 1:10 in 9 mL LB Kan in a 125 mL flask and grown overnight at 37°C while shaking at 200 RPM. The next day, the culture was used to inoculate 400 mL of LB Kan at a starting OD_{600} of 0.1 and grown at 30°C until the OD_{600} reached between 0.6 and 0.7, at which point IPTG was added at a final concentration of 1 mM and the culture was moved to 16°C with shaking at 160 RPM for 16 hours. For purification, slight modifications to the lysis buffer and elution buffers were made. Frozen pellets of PchR-SUMO and AbrB-SUMO were resuspended in 40 mL lysis buffer (50 mM Tris pH 8, 500 mM NaCl, 10% glycerol, 20 mM imidazole, supplemented with 1 EDTA-free protease inhibitor tablet), lysed by sonication, and the lysate cleared by

centrifugation. Clarified lysate was applied to 3 mL Ni-NTA resin columns, the columns were washed with 60 mL lysis buffer, and proteins were eluted by step elution using 5 mL each of increasing imidazole concentrations (elution buffer: 50 mM Tris pH 8, 500 mM NaCl, 10% glycerol, imidazole at 50, 100, 200, and 350 mM). Elution fractions were assayed for relative protein concentration by the Bradford assay (BioRad) and fractions containing protein were electrophoresed on SDS-PAGE to ensure proper expression and purification. Removal of the SUMO tag and purification of SUMO-free protein was carried out as described above. SUMO-free AbrB required an additional anion exchange purification step using a HiTrap qFF (Cytivia 17515601) anion exchange column attached to an AKTA FPLC. The column was equilibrated with 10% Q Buffer B (50 mM Tris, 5% glycerol, and 500 mM NaCl). Sumo-free AbrB was diluted to 50 mM NaCl in Q Buffer A and loaded into the column. Protein fractions (2 mL) were collected as the system increased the percentage of Q Buffer B while monitoring A260 readings. High A260 peaks were measured for AbrB on SDS-PAGE and correct fractions were pooled, dialyzed, concentrated by dialysis, mixed with glycerol at 25% final concentration, and stored at -80C.

Electrophoretic Mobility Shift Assays

5′ IRDye® 700-labeled probes of the *yvmC* promoter (-244 to +9 relative to the ATG start codon) were generated by PCR using the primer pair oNLF433-oNLF387 using pNF035 as a template. PCR products were purified by gel extract and quantified by nanodrop. To generate the *P*yvmCΔ59 probe, two PCR reactions were carried out with primer pairs oLVG025A-oNLF467 and oNLF468-oNLF387. The two PCR products were gel extracted and fused together by SOE PCR (see Cloning). The fragment was then used as template

for PCR with primer pairs oNLF433-oNLF387, resulting in a 5′ IRDye® 700 labeled DNA fragment lacking 59-bp. Binding reactions were assembled by first generating a binding solution: 1X binding buffer (5X binding buffer: 250 mM Tris pH 8, 5 mM EDTA, 150 mM KCl, 10 mM $MgCl_2$, 12.5 mM DTT, 1.25% Tween 20, and 2.5 mg/mL BSA), 1X DNA probe (10X probe, 100 nM), 1 µL protein of interest (5X stock concentration), and water up to 5 µL. The binding reactions were incubated for 30 minutes at 37°C. When indicated, 1 µL of 1X heparin (6X heparin: 0.06 mg/mL) was added to each reaction after incubation and 3 µL were loaded into the wells of a 15-well 6% polyacrylamide gel and ran for 60 minutes at 150V at room temperature. After gel electrophoresis, the gels were left in the glass plates and imaged using an Odyseey xCl imager (1.5 mm offset height, 84 µm resolution). The resulting images were adjusted in Fiji [26] and cropped and annotated in Adobe Illustrator®. EMSA experiments were carried out at least three times with separate aliquots for each protein.

Fluorescent DNAse I and Differential Peak Height Analysis

5′ FAM-labeled probes were generated by PCR using the primer pair oNLF432-oNLF387 using pNF035 as a template. PCR products were purified by gel extraction and quantified by nanodrop. Binding reactions were assembled and carried out identically to EMSA experiments. After incubation, 1 µL 0.6 mg/mL heparin, and 0.79 µL of 10X DNAse I buffer (Invitrogen) were added to the binding reactions followed by 1.2 µL of diluted DNAse I (0.625 U total, Invitrogen) and reactions were incubated at room temperature for 5 minutes. After 5 minutes, reactions were heated to 72°C for 10 minutes and DNA was immediately purified by phenol-chloroform extraction and ethanol precipitation. Reactions were resuspended in 10 µL water (company) and submitted for fragment

371 analysis by Azenta®. The resulting.fa files were imported into R and the data aligned to
372 the LIZ500 reference standards using the *storing.inds* and *overview* functions from the R
373 package Fragman [27]. To analyze differences between peak heights, the R function
374 findPeaks was used to extract local maxima in the sequential peak height data [28].
375 Differential peak height analysis was carried out as described in [29]. Briefly, the raw
376 signal for each sample was normalized by dividing by the sum of all signals. Then, the
377 normalized signal for the sample incubated with protein was subtracted from the signal
378 incubated without protein, producing the differential peak height. DNAse I protection
379 produces negative values while DNAse I hypersensitivity produces positive values.
380 DNAse I footprinting and differential peak height analysis were carried out at least twice
381 with separate protein aliquots.
382

Results

ScoC Negatively Regulates Pulcherrimin Production

The TSR ScoC represses gene expression during exponential phase [5,10,30]. As nutrients become limiting, the effect of ScoC repression is lessened by downregulation of *scoC* expression and competition between other DNA binding proteins [10,30,31]. Our lab has identified ScoC as a methylation-responding transcription factor at a promoter of a gene not involved in protease production, thus we were interested in further characterizing the role of ScoC as a TSR in *B. subtilis* [25]. When culturing our WT strain (DK1042) to late stationary phase cultures appear grey in liquid minimal media (Tris-Spizizen Salts, TSS) and appear red on TSS agar **(Fig. 1).** An isogenic *scoC* disruption mutant (*scoC::*erm), interestingly, appears pink in liquid TSS and has a more intense coloring when grown on solid TSS plates compared to WT **(Fig. 1).** The red phenotype was 1) dependent on the amount of $FeCl_3$, 2) not present on standard LB plates, and 3) present on LB plates supplemented with $FeCl_3$ **(S1 Fig.)**. Thus, excess iron was responsible for the red phenotype.

B. subtilis and many other microorganisms produce and secrete the iron chelator pulcherriminic acid, which binds to free ferric iron to form the insoluble pigment pulcherrimin [14,15,32] **(Fig. 6A)**. We hypothesized that the red phenotype was caused by the production of pulcherrimin. Therefore, we made mutations in one the two key pulcherrimin biosynthetic genes (*yvmC*) in the WT and *scoC::erm* backgrounds. After growth in liquid and on solid media, the red phenotype in the mutants lacking *yvmC* was absent**,** indicating pulcherrimin is responsible for the red phenotype in both the WT and *scoC::erm* backgrounds (**Fig. 1)**. Additionally, mass spectrometry analysis of cyclo(L-

406 leucine-L-leucie) (cLL), a pulcherriminic acid precursor synthesized by the cyclization of
407 tRNA-charged leucine by YvmC, showed that mutants lacking *yvmC* no longer have
408 detectable cLL **(S2 Fig.).** Further, complementing the *scoC::erm* by ectopically expressing
409 *scoC* from its native promoter causes the red phenotype to disappear **(S3 Fig.).** Together,
410 our results indicate that ScoC negatively controls pulcherriminic acid production, in turn
411 resulting in increased extracellular pulcherrimin and the red color in TSS media.

412 **Multiple Systems Control Pulcherrimin Production in *B. subtilis.***

413 Past studies have identified AbrB, another TSR, as a regulator of pulcherrimin
414 production in *B. subtilis* and *Bacillus licheniformis* [9,15]. We therefore generated an *abrB*
415 disruption strain (*abrB::kan*) and assessed pigment formation after overnight growth. Like
416 *scoC::erm,* the liquid media turned slightly pink relative to WT. On solid media, *abrB::kan*
417 appeared wrinkly and was less red than *scoC::erm* and more red than WT **(Fig. 1)**. The
418 wrinkly phenotype of *abrB::kan* colonies is due to its role in negatively regulating biofilm
419 formation [33].

420 Many bacteria that encode the pulcherriminic acid biosynthesis genes also encode
421 the negative regulator *pchR* which inhibits expression of the biosynthesis operon [12]. In
422 *B. subtilis,* mutants lacking *pchR* appear red in liquid culture after overnight growth in
423 minimal media (MS media) [13]. Indeed, deletion of *pchR* (Δ*pchR*) resulted in a more
424 intense red coloring of the liquid and solid TSS media compared to WT and the other
425 single mutants **(Fig. 1)**. Combining the mutations in the same background, resulting in
426 three double-mutants and one triple mutant, results in a color intensity higher than any
427 single mutant alone **(Fig. 1).** However, whether there are differences in the amount, or
428 even the rate at which pulcherrimin produced, is not easily determined with qualitative

comparisons, necessitating a quantitative assessment of pulcherrimin production during a growth curve (see below).

ScoC, AbrB, and PchR Control the Timing, Rate, and Amount of Pulcherrimin Produced in Liquid Cultures.

Iron bound pulcherriminic acid (pulcherrimin) is water-insoluble at neutral pH and can be sedimented with cells through centrifugation and solubilized in a basic solution (2 mM NaOH). In this solution, pulcherrimin can be analyzed spectrophotometrically with peak absorbances at 245, 285, and 410 nm [16,34]. Therefore, the amount of pulcherrimin produced in a culture growing over time can be determined by measuring the absorbance at 410 nm (A_{410}) from alkali-solubilized cell pellets. We were interested in how pulcherrimin production changed as cells transitioned from exponential growth to stationary phase. Therefore, we measured the absorbance at 410 nm (A_{410}) in the WT background and found that it rose steadily throughout the growth curve, plateauing at 0.10 after 18 hours post transition into stationary phase **(Fig. 2A)**. Interestingly, the A_{410} in the *yvmC::erm* background, which lacks an enzyme necessary for the pulcherrimin precursor cLL, is indistinguishable from WT **(S2 Fig., Fig. 2A)**. These data demonstrate pulcherrimin production in the WT background grown in liquid TSS culture is below the limit of detection for this assay and that the A_{410} in WT and *yvmC::erm* represents the background absorbance.

We repeated this experiment with all strains and analyzed the data using a growth model to estimate the start time, the duration, the rate, and the maximum amount of pulcherrimin produced **(Fig. 2AB).** Genes controlled by TSRs tend to have low expression during exponential phase and higher expression as cells transition into stationary phase

[2,10,31,35–37]. We hypothesized that the effect of *scoC* and *abrB* disruption would cause increased pulcherrimin production as cells transition into stationary phase while cells without *pchR* would have higher pulcherrimin production during exponential phase. Compared to any single mutant, Δ*pchR* had the earliest production start time while *abrB::erm* began pulcherrimin production just prior to the start of the transition phase **(Fig. 2A, Bi).** The maximum production rate and duration of pulcherrimin production were similar across all single mutants while Δ*pchR* had the highest maximum A_{410} **(Fig 2Bi-iv)**. The data from the single mutants suggests *pchR* is a potent repressor of pulcherrimin production, especially during exponential phase while *scoC* and *abrB* contribute to repress production during late exponential through early stationary phase.

We next were interested in how combining mutations to generate double and triple mutants affected pulcherrimin production parameters. When comparing against the single mutants, combining *scoC::erm* and *abrB::kan* resulted in a production start time and production duration comparable to the single *scoC* disruption **(Fig. 2Bi-ii).** However, the *scoC::erm abrB::kan* background had an increased pulcherrimin production rate and a maximum A_{410} much higher than the single mutants, demonstrating positive epistasis **(Fig. 2Biii-iv, S4 Fig.).** Introducing *scoC::erm* or *abrB::kan* into the Δ*pchR* background generated strains with production start times and pulcherrimin production durations similar to Δ*pchR* **(Fig. 2Bi).** While the maximum production rate was higher in Δ*pchR scoC::erm* than Δ*pchR abrB::kan*, the maximum A_{410} were similar **(Fig. 2Biii-iv).** This can be reconciled by the fact that Δ*pchR abrB::kan* has a longer duration of pulcherrimin production than Δ*pchR scoC::erm* **(Fig. 2Bii)**. In the triple mutant background, pulcherrimin production began at the first sampled timepoint, six hours before the

transition into stationary phase, demonstrating all transcription factors contribute to inhibiting expression during exponential phase **(Fig. 2A, Bi).** The triple mutant had the longest duration of pulcherrimin production of all mutants tested while the maximum production rate was lower than most double mutants and similar to all single mutants. Despite the lower production rate, the maximum A_{410} was similar to or higher than all double mutants, likely because of the extended production period **(Fig. 2Bii-iv).** Taken together, the results indicate multiple transcription factors control the rate, duration, and maximum amount of pulcherrimin produced and demonstrate an integration of multiple regulatory systems on an energetically costly phenotype.

The *yvmC* Promoter is Upregulated in the Absence of ScoC, AbrB, and PchR.

As transcription factors, we hypothesized the main role of ScoC, AbrB, and PchR in controlling pulcherrimin formation likely involves regulating promoter activity. We therefore fused the promoter for *yvmC* (P_{yvmC}) to GFP and measured single-cell fluorescence via flow cytometry during early exponential phase (approximately 3 hours before T0). 69.8% (+/- 9.87%) of the WT population were GFP positive compared to a no GFP control **(Fig. 3A).** The percent positive population of cells in the *scoC::erm* and *abrB::kan* backgrounds were greater than WT. Further, the wider distribution of fluorescence intensities indicate a broader range of expression levels within the population compared to WT. We found a proportional relationship between maximum A_{410} values and reporter expression for most strains **(Fig. 2Biv, Fig. 3).** Additionally, mutants with higher reporter activity tend to have more narrow fluorescence distributions **(Fig. 3).** After many attempts, we were unable to generate a strain harboring the reporter in the *scoC::erm abrB::kan* double mutant background. Indeed, mutants of *scoC* and *abrB* have

498 decreased expression of the competence regulator *comK* and have decreased
499 competence compared to WT [7,38]. Together, our results demonstrate PchR, ScoC, and
500 AbrB work to inhibit expression of the pulcherrimin biosynthesis genes *yvmC* and *cypX*
501 and that increased promoter expression results in increased pulcherrimin production.

502 **Analysis of Transcription Factor Binding at the *yvmC* Promoter.**

503 Randazzo and coworkers aligned promoter regions of PchR regulated genes and
504 identified a 14-bp consensus sequence termed the PchR-box [13]. To validate their in
505 silico consensus motif, we utilized fluorescent DNAse I footprinting assays followed by
506 differential peak height analysis to identify the PchR binding site in vitro. PchR
507 demonstrated a protected region from +6 to +28 relative to the transcriptional start site
508 (determined by [39]), which overlaps with the previously identified PchR-box **(Fig. 4Ai-ii,**
509 **[13]).** We repeated this experiment with purified AbrB and ScoC. We found that AbrB had
510 a broad protection area encapsulating -30 to approximately +60 bp relative to the
511 transcriptional start site **(Fig. 4B). While broader than PchR, the protection region of**
512 **AbrB is consistent with earlier reports of AbrB-DNA interactions [40].** Interestingly,
513 attempts at DNAse I footprinting analysis with ScoC and the *yvmC* promoter were
514 unsuccessful, with no apparent difference in peak heights between samples with and
515 without protein **(S5A Fig.).** During optimization experiments, we found that ScoC could
516 bind to the *yvmC* promoter when the non-specific competitor poly dI-dC was used, rather
517 than the polyanionic compound heparin used in experiments with PchR and AbrB. We
518 therefore analyzed the DNAse I footprint with ScoC using poly dI-dC as a non-specific
519 competitor and observed a broad protection area from approximately -10 to + 60 relative
520 to the transcriptional start site **(Fig. 4C)**.

The footprint data indicated all proteins interacted with the *yvmC* promoter downstream of the putative SigA binding site **(Fig. 6B).** We therefore generated a mutant probe where 59 base pairs, from -14 to +45 bp, were deleted (Δ59) and assessed DNA binding in vitro by electrophoretic mobility shift assays (EMSA) using the WT and Δ59 probes. PchR exhibited the most canonical behavior of the transcription factors, demonstrating discrete band formation as protein concentration increased **(Fig. 5A).** At the highest concentration tested, PchR formed a second DNA-bound species that migrated slower than the other band formed at lower concentrations, suggesting an additional, low-affinity site may be present in the promoter (**Fig. 5A).** However, DNAse I footprinting analysis identified only one area of protection, suggesting the slow-migrating complex may be caused by non-specific interactions between PchR and DNA at the high protein concentration **(Fig. 4A).** Indeed, when using the Δ59 probe, which lacks the region recognized by PchR, there is a faint shift at the highest PchR concentration **(Fig. 5B).** This suggests that high PchR concentrations can interact with the *yvmC* promoter non-specifically but demonstrates specific binding at lower concentrations. For AbrB, the intensity of the unbound probe decreased as protein concentration increased, indicating that DNA binding is occurring. However, the lack of discrete bands indicate the AbrB-*PyvmC* interaction likely represent a fast off-rate **(Fig. 5A**). Additionally, protein binding was not observed in experiments using the Δ59 probe **(Fig. 5Bi).** ScoC had smear shifts at concentrations greater than 250 nM with a band present at 1000 nM **(Fig. 5A)**. Interestingly, a band was also present at 1000 nM when using the Δ59 probe but not ant 250 or 500 nM, suggesting binding at 1000 nM occurs non-specifically **(Fig. 5B).** Previous studies of in vitro ScoC-DNA interactions found that ScoC binds to DNA non-specifically

544 at concentrations greater than 400 nM and the DNAse I footprint size is around 14-25 bps
545 [30]. The fact that ScoC bound to the WT probe but not the Δ59 probe indicates specificity,
546 but it is apparent that the ScoC-*yvmC* interaction likely has a fast off-rate as suggested
547 with AbrB. Nonetheless, the results indicate the PchR and AbrB, collectively, act as road-
548 blocks to RNAP progression at the *yvmC* promoter while the role of ScoC appears to
549 involve weak direct regulation and may also have indirect regulation through another
550 factor that ScoC modulates. Taken together, the presence of the three repressors is
551 necessary to limit the production of pulcherrimin providing mechanistic insight into the
552 regulatory network of pulcherrimin production in bacteria.

553 **Discussion**

554 In *B. subtilis,* seemingly redundant regulatory pathways are abundant. In this
555 study, we uncover the layered negative regulation of the iron chelator pulcherrimin by two
556 discrete regulatory systems. We demonstrate that these systems work together to inhibit
557 the biosynthetic pathway of an energetically costly and potentially growth limiting
558 metabolite. While expression patterns of *yvmC*-GFP promoter fusion closely resembled
559 the pattern of pulcherrimin production, the reporter in the *scoC::erm* and *abrB::kan*
560 background displayed broad distributions of promoter expression, suggesting the TSRs
561 influence heterogeneity in pulcherrimin producing cells. Only in the absence of all three
562 transcription factors is *yvmC* gene expression fully relieved and pulcherrimin is produced
563 throughout exponential phase. Our biochemical analysis shows the regulator of the
564 pulcherrimin biosynthesis operon and the transition state regulators ScoC and AbrB bind
565 to the *yvmC* promoter with differing apparent off-rates. Together, our results indicate

pulcherrimin regulation in *Bacillus subtilis* is under tight regulation and repressed during exponential growth by two distinct regulatory systems.

The transition state regulators ScoC and AbrB have been subject to much research for their roles in diverse aspects of *Bacillus* physiology. The absence of these regulators modifies sporulation, competence, protease production, and biofilm formation among many other phenotypes [7,10,35,37,41–44]. Microarray analysis of the effect of *scoC* on global gene expression was carried out from cells sampled at different points in the growth cycle in complex media [7]. While hundreds of genes were found to be differentially regulated in the Δ*scoC* background, expression of genes involved in pulcherrimin biosynthesis were not identified as significantly different from the WT background [7]. This could be due to the rich, complex media used during the experiment, as *B. subtilis* grown in media with certain amino acids present have lower levels of *scoC* expression compared to media without amino acids [10,30]. In rich media, the GTP/amino acid-sensing transcriptional regulator CodY is active and negatively regulates *scoC* expression [10,30,45].Under the conditions used for experiments here, the lack of amino acids as a nitrogen source means CodY is mostly in the inactive state and *scoC* expression is elevated. Elevated *scoC* could explain how *yvmC* gene expression and pulcherrimin production is near background levels in WT cells **(Fig. 2 and 3).**

The major extracellular proteases AprE and NprE are transcriptionally regulated by ScoC and AbrB [10]. Promoter expression of *aprE* and *nprE* in TSS media is elevated above WT in Δ*scoC* and Δ*abrB* but is similar between the two mutants. Expression increases beyond expected when *scoC* and *abrB* mutations are combined, similar to the effect size observed in pulcherrimin production **(Fig. 2, [10]).** While *abrB* has been

589 described as a negative regulator of *scoC* expression, experiments in TSS media found
590 no effect of an *abrB* mutant on *scoC* promoter expression [2,30]. Thus, the effect of the
591 double *scoC abrB* mutant on *aprE* and *nprE* expression was attributed to the lack of direct
592 regulation by CodY, which is inactive in TSS media without amino acid supplementation
593 [10]. The promoter region of *yvmC* does not have a CodY binding site nor is there
594 evidence CodY binds to the *yvmC* promoter in vivo [10,30,45]. Therefore, the effect of
595 CodY on pulcherrimin production likely occurs indirectly through regulation of ScoC,
596 similar to regulation of the peptide transporter gene *dtpT* [30].

597 In addition to evidence that AbrB directly controls *yvmC* expression in *B. subtilis,*
598 AbrB was also identified as a direct regulator of pulcherrimin biosynthesis in *B.*
599 *licheniformis* [9,11,15]. Interestingly, the *abrB* deletion had a larger effect on maximum
600 pulcherrimin production in *B. licheniformis* than in *B. subtilis,* indicating that despite similar
601 regulatory components, their effects appear species specific [15]. Further, the homolog
602 for *pchR* is not located adjacent to the pulcherrimin biosynthesis gene cassette like *B.*
603 *subtilis* (**Fig. 6B)**. A neighboring MarR-family transcription factor YvnA was also identified
604 as a regulator of pulcherrimin biosynthesis in *B. licheniformis*, where it bound directly to
605 the intergenic region between *yvmA* and *yvmC* [15]. One possibility is that the different
606 genetic organizations of the pulcherrimin biosynthetic gene cassette may necessitate
607 alternative forms of regulation, thus explaining the difference between *B. licheniformis*
608 and *B. subtilis.*

609 In *B. subtilis,* the *pchR* gene is located adjacent to *yvmA* and divergently
610 transcribed from *yvmC-cypX* **(Fig. 6B)** and binds to a consensus motif (PchR-box)
611 upstream of *yvmC.* Our footprinting analysis identified the same region protected from

612 DNase treatment, validating the predicted motif [13]. MarR family transcription factors
613 commonly bind to small ligands which alter their DNA binding capabilities [46]. ZitR, a
614 Zn^{2+}-binding MarR transcription factor from *Lactococcus lactis*, is the template for PchR
615 homology modeling by Phyre2 [47]. In the cytosol, iron species tend to be in the reduced
616 Fe^{2+} state, thus it is tempting to hypothesize that ferrous iron is the ligand to inhibit PchR
617 repression [48]. However, several lines of evidence indicate iron is not directly involved
618 in pulcherriminic acid production. For example, *B. subtilis* grown in minimal media
619 supplemented with very low iron (0.0001 w/v% ferric ammonium citrate), produced no
620 pigment after overnight growth [49]. Yet, pigment formed with peak absorbance at 410
621 nm after supplementation of ferric ammonium citrate crystals directly to culture, indicating
622 pulcherriminic acid is produced despite the low levels of iron in the growth medium [49].
623 Further, work from Angelini and coworkers demonstrated the *yvmC* promoter activity is
624 not responsive to iron supplementation [50]. Thus, the ligand for PchR, if it exists, has
625 yet to be determined but would provide insight into conditions that favor pulcherrimin
626 production.

627 Why *B. subtilis* and other organisms produce pulcherrimin is a topic of interest.
628 Recent studies found that *B. subtilis* in biofilms produce pulcherrimin as a form of niche
629 protection by creating a zone of iron limitation around the biofilm [12]. Other groups found
630 that pulcherrimin production increased resistance to reactive oxygen species (ROS),
631 likely by decreasing the amount of iron available for Fenton reactions [50,51]. The role of
632 an antioxidant is interesting given that stationary phase cells tend to be more tolerant to
633 hydrogen peroxide than cells in exponential phase independent of prior exposure to ROS
634 [52]. Additionally, production of the cytosolic mini-ferritin MrgA is increased as cells

transition into stationary phase in a mechanism independent of TSRs [53]. As a Dps homolog, MrgA is predicted to sequester iron and enzymatically oxidize Fe(II) to the insoluble and less reactive Fe(III) [54]. Thus, control of pulcherrimin production by TSRs agrees with a model wherein intracellular and extracellular iron is sequestered as cells enter stationary phase, limiting proliferation of reactive oxygen species.

Acknowledgements

We would like to thank members of the Simmons lab for helpful discussions during the progression of this work, the Michigan State University Mass Spectrometry and Metabolomics Core for quantitative measurements of intracellular cyclo-(L-leucine-L-leucine), and J.M. Fernandez for constructing the light box used to image agar plates. This work was supported by grant 1R35GM131772 from the National Institutes of Health to LAS and by an NSF PRFB award (2010735).

References

1. Zeigler DR. The Bacillus Genetic Stock Center/*Bacillus subtilis*. 1st ed. In: Jarret RL, McCluskey K, editors. The Biological Resources of Model Organisms. 1st ed. Boca Raton, Florida : CRC Press, [2019]: CRC Press; 2019. pp. 35–53. doi:10.1201/9781315100999-3

2. Perego M, Hoch JA. Sequence analysis and regulation of the *hpr* locus, a regulatory gene for protease production and sporulation in <i>Bacillus subtilis<i/>. J Bacteriol. 1988;170: 2560–2567. doi:10.1128/jb.170.6.2560-2567.1988

3. Strauch MA, Hoch JA. Biology of Bacilli. Butterworth; 1991. pp. 105–121.

4. Strauch MA, Hoch JA. Transition-state regulators: sentinels of *Bacillus subtilis* post-exponential gene expression. Mol Microbiol. 1993;7: 337–342. doi:10.1111/j.1365-2958.1993.tb01125.x

5. Higerd TB, Hoch JA, Spizizen J. Hyperprotease-Producing Mutants of *Bacillus subtilis*. J Bacteriol. 1972;112: 1026–1028. doi:10.1128/jb.112.2.1026-1028.1972

6. Kallio PT, Fagelson JE, Strauch MA. The Transition State Regulator Hpr of *Bacillus subtilis* Is a DNA-binding Protein. The Journal of Biological Chemistry. 1991;226: 13411–13417.

7. Caldwell R, Sapolsky R, Weyler W, Maile RR, Causey SC, Ferrari E. Correlation between *Bacillus subtilis scoC* Phenotype and Gene Expression Determined Using Microarrays for Transcriptome Analysis. Journal of Bacteriology. 2001;183: 7329–7340. doi:10.1128/JB.183.24.7329-7340.2001

8. Coles M, Djuranovic S, Söding J, Frickey T, Koretke K, Truffault V, et al. AbrB-like Transcription Factors Assume a Swapped Hairpin Fold that Is Evolutionarily Related to Double-Psi β Barrels. Structure. 2005;13: 919–928. doi:10.1016/j.str.2005.03.017

9. Chumsakul O, Takahashi H, Oshima T, Hishimoto T, Kanaya S, Ogasawara N, et al. Genome-wide binding profiles of the Bacillus subtilis transition state regulator AbrB and its homolog Abh reveals their interactive role in transcriptional regulation. Nucleic Acids Research. 2011;39: 414–428. doi:10.1093/nar/gkq780

10. Barbieri G, Albertini AM, Ferrari E, Sonenshein AL, Belitsky BR. Interplay of CodY and ScoC in the Regulation of Major Extracellular Protease Genes of *Bacillus subtilis*. Henkin TM, editor. Journal of Bacteriology. 2016;198: 907–920. doi:10.1128/JB.00894-15

11. Chumsakul O, Nakamura K, Kurata T, Sakamoto T, Hobman JL, Ogasawara N, et al. High-Resolution Mapping of In vivo Genomic Transcription Factor Binding Sites Using In situ DNase I Footprinting and ChIP-seq. DNA Research. 2013;20: 325–338. doi:10.1093/dnares/dst013

12. Arnaouteli S, Matoz-Fernandez DA, Porter M, Kalamara M, Abbott J, MacPhee CE, et al. Pulcherrimin formation controls growth arrest of the *Bacillus subtilis* biofilm. Proc Natl Acad Sci USA. 2019;116: 13553–13562. doi:10.1073/pnas.1903982116

13. Randazzo P, Aubert-Frambourg A, Guillot A, Auger S. The MarR-like protein PchR (YvmB) regulates expression of genes involved in pulcherriminic acid biosynthesis and in the initiation of sporulation in *Bacillus subtilis*. BMC Microbiol. 2016;16: 190. doi:10.1186/s12866-016-0807-3

14. Krause DJ, Kominek J, Opulente DA, Shen X-X, Zhou X, Langdon QK, et al. Functional and evolutionary characterization of a secondary metabolite gene cluster in budding yeasts. Proc Natl Acad Sci USA. 2018;115: 11030–11035. doi:10.1073/pnas.1806268115

15. Wang D, Zhan Y, Cai D, Li X, Wang Q, Chen S. Regulation of the Synthesis and Secretion of the Iron Chelator Cyclodipeptide Pulcherriminic Acid in *Bacillus licheniformis*. Drake HL, editor. Appl Environ Microbiol. 2018;84: e00262-18. doi:10.1128/AEM.00262-18

16. Kluyver AJ, Van Der Walt JP, Van Triet AJ. Pulcherrimin, The Pigment of *Candida Pulcherrima*. Proc Natl Acad Sci USA. 1953;39: 583–593. doi:10.1073/pnas.39.7.583

17. Konkol MA, Blair KM, Kearns DB. Plasmid-Encoded ComI Inhibits Competence in the Ancestral 3610 Strain of *Bacillus subtilis*. Journal of Bacteriology. 2013;195: 4085–4093. doi:10.1128/JB.00696-13

18. Koo B-M, Kritikos G, Farelli JD, Todor H, Tong K, Kimsey H, et al. Construction and Analysis of Two Genome-Scale Deletion Libraries for *Bacillus subtilis*. Cell Systems. 2017;4: 291-305.e7. doi:10.1016/j.cels.2016.12.013

19. Routh S, Acharyya A, Dhar R. A two-step PCR assembly for construction of gene variants across large mutational distances. Biology Methods and Protocols. 2021;6: bpab007. doi:10.1093/biomethods/bpab007

20. Trauth S, Bischofs IB. Ectopic Integration Vectors for Generating Fluorescent Promoter Fusions in *Bacillus subtilis* with Minimal Dark Noise. Scheffers D-J, editor. PLoS ONE. 2014;9: e98360. doi:10.1371/journal.pone.0098360

21. Smith P, Schuster M. Inexpensive Apparatus for High-Quality Imaging of Microbial Growth on Agar Plates. Front Microbiol. 2021;12: 689476. doi:10.3389/fmicb.2021.689476

22. Pisithkul T, Schroeder JW, Trujillo EA, Yeesin P, Stevenson DM, Chaiamarit T, et al. Metabolic Remodeling during Biofilm Development of *Bacillus subtilis*. Ghigo J-M, Greenberg EP, editors. mBio. 2019;10: e00623-19. doi:10.1128/mBio.00623-19

23. Hall BG, Acar H, Nandipati A, Barlow M. Growth Rates Made Easy. Molecular Biology and Evolution. 2014;31: 232–238. doi:10.1093/molbev/mst187

24. Baier F, Gauye F, Perez-Carrasco R, Payne JL, Schaerli Y. Environment-dependent epistasis increases phenotypic diversity in gene regulatory networks. SCIENCE ADVANCES. 2023.

25. Nye TM, van Gijtenbeek LA, Stevens AG, Schroeder JW, Randall JR, Matthews LA, et al. Methyltransferase DnmA is responsible for genome-wide N6-methyladenosine modifications at non-palindromic recognition sites in *Bacillus subtilis*. Nucleic Acids Research. 2020;48: 5332–5348. doi:10.1093/nar/gkaa266

26. Schindelin J, Arganda-Carreras I, Frise E, Kaynig V, Longair M, Pietzsch T, et al. Fiji: an open-source platform for biological-image analysis. Nature Methods. 2012;9: 676–682. doi:10.1038/nmeth.2019

27. Covarrubias-Pazaran G, Diaz-Garcia L, Schlautman B, Salazar W, Zalapa J. Fragman: an R package for fragment analysis. BMC Genet. 2016;17: 62. doi:10.1186/s12863-016-0365-6

28. Grinberg S. findPeaks. Available: https://github.com/stas-g/findPeaks

29. Davlieva M, Shi Y, Leonard PG, Johnson TA, Zianni MR, Arias CA, et al. A variable DNA recognition site organization establishes the LiaR-mediated cell envelope stress response of enterococci to daptomycin. Nucleic Acids Research. 2015;43: 4758–4773. doi:10.1093/nar/gkv321

30. Belitsky BR, Barbieri G, Albertini AM, Ferrari E, Strauch MA, Sonenshein AL. Interactive regulation by the *Bacillus subtilis* global regulators CodY and ScoC. Molecular Microbiology. 2015;97: 698–716. doi:10.1111/mmi.13056

31. Ogura M, Matsuzawa A, Yoshikawa H, Tanaka T. *Bacillus subtilis* SalA (YbaL) Negatively Regulates Expression of *scoC*, Which Encodes the Repressor for the Alkaline Exoprotease Gene, *aprE*. Journal of Bacteriology. 2004;186: 3056–3064. doi:10.1128/JB.186.10.3056-3064.2004

32. Uffen RL, Canale-Parola E. Synthesis of Pulcherriminic Acid by *Bacillus subtilis*. J Bacteriol. 1972;111: 86–93. doi:10.1128/jb.111.1.86-93.1972

33. Hamon MA, Lazazzera BA. The sporulation transcription factor Spo0A is required for biofilm development in *Bacillus subtilis*. Molecular Microbiology. 2001;42: 1199–1209. doi:10.1046/j.1365-2958.2001.02709.x

34. Canale-Parola E. A red pigment produced by aerobic sporeforming bacteria. Archiv für Mikrobiologie. 1963; 414–417.

35. Kaushal B, Paul S, Hulett FM. Direct Regulation of *Bacillus subtilis phoPR* Transcription by Transition State Regulator ScoC. Journal of Bacteriology. 2010;192: 3103–3113. doi:10.1128/JB.00089-10

36. Kodgire P, Rao KK. *hag* expression in *Bacillus subtilis* is both negatively and positively regulated by ScoC. Microbiology. 2009;155: 142–149. doi:10.1099/mic.0.021899-0

37. Koide A, Perego M, Hoch JA. ScoC Regulates Peptide Transport and Sporulation Initiation in *Bacillus subtilis*. 1999;181: 4.

38. Hahn J, Luttinger A, Dubnau D. Regulatory inputs for the synthesis of ComK, the competence transcription factor of *Bacillus subtilis*. Molecular Microbiology. 1996;21: 763–775. doi:10.1046/j.1365-2958.1996.371407.x

39. Zhu B, Stülke J. SubtiWiki in 2018: from genes and proteins to functional network annotation of the model organism *Bacillus subtilis*. Nucleic Acids Research. 2018;46: D743–D748. doi:10.1093/nar/gkx908

40. Strauch MA, Spiegelman GB, Perego M, Johnson WC, Burbulys D, Hoch JA. The transition state transcription regulator *abrB* of *Bacillus subtilis* is a DNA binding protein. The EMBO Journal. 1989;8: 1615–1621. doi:10.1002/j.1460-2075.1989.tb03546.x

41. Bobay BG, Benson L, Naylor S, Feeney B, Clark AC, Goshe MB, et al. Evaluation of the DNA Binding Tendencies of the Transition State Regulator AbrB. Biochemistry. 2004;43: 16106–16118. doi:10.1021/bi048399h

42. Bochmann SM, Spieß T, Kötter P, Entian K-D. Synthesis and Succinylation of Subtilin-Like Lantibiotics Are Strongly Influenced by Glucose and Transition State Regulator AbrB. Drake HL, editor. Appl Environ Microbiol. 2015;81: 614–622. doi:10.1128/AEM.02579-14

43. Hamoen LW, Kausche D, Marahiel MA, Sinderen D, Venema G, Serror P. The *Bacillus subtilis* transition state regulator AbrB binds to the −35 promoter region of *comK*. FEMS Microbiology Letters. 2003;218: 299–304. doi:10.1111/j.1574-6968.2003.tb11532.x

44. Inaoka T, Wang G, Ochi K. ScoC Regulates Bacilysin Production at the Transcription Level in *Bacillus subtilis*. Journal of Bacteriology. 2009;191: 7367–7371. doi:10.1128/JB.01081-09

45. Belitsky BR, Sonenshein AL. Genome-wide identification of *Bacillus subtilis* CodY-binding sites at single-nucleotide resolution. Proc Natl Acad Sci USA. 2013;110: 7026–7031. doi:10.1073/pnas.1300428110

46. Deochand DK, Grove A. MarR family transcription factors: dynamic variations on a common scaffold. Critical Reviews in Biochemistry and Molecular Biology. 2017;52: 595–613. doi:10.1080/10409238.2017.1344612

47. Kelley LA, Mezulis S, Yates CM, Wass MN, Sternberg MJE. The Phyre2 web portal for protein modeling, prediction and analysis. Nat Protoc. 2015;10: 845–858. doi:10.1038/nprot.2015.053

48. Helmann JD. Specificity of Metal Sensing: Iron and Manganese Homeostasis in *Bacillus subtilis*. Journal of Biological Chemistry. 2014;289: 28112–28120. doi:10.1074/jbc.R114.587071

49. Kupfer DG, Uffen RL, Canale-Parola E. The Role of Iron and Molecular Oxygen in Puleherrimin Synthesis by Bacteria. Archiv für Mikrobiologie. 1967; 9–21.

50. Angelini LL, Dos Santos RAC, Fox G, Paruthiyil S, Gozzi K, Shemesh M, et al. Pulcherrimin protects *Bacillus subtilis* against oxidative stress during biofilm development. npj Biofilms Microbiomes. 2023;9: 50. doi:10.1038/s41522-023-00418-z

51. Charron-Lamoureux V, Haroune L, Pomerleau M, Hall L, Orban F, Leroux J, et al. Pulcherriminic acid modulates iron availability and protects against oxidative stress during microbial interactions. Nat Commun. 2023;14: 2536. doi:10.1038/s41467-023-38222-0

52. Dowds BCA, Hoch JA. Regulation of the oxidative stress response by the *hpr* gene in *Bacillus subtilis*. Journal of General Microbiology. 1991;137: 1121–1125. doi:10.1099/00221287-137-5-1121

53. Chen L, James LP, Helmann JD. Metalloregulation in *Bacillus subtilis*: isolation and characterization of two genes differentially repressed by metal ions. J Bacteriol. 1993;175: 5428–5437. doi:10.1128/jb.175.17.5428-5437.1993

54. Orban K, Finkel SE. Dps Is a Universally Conserved Dual-Action DNA-Binding and Ferritin Protein. Maupin-Furlow JA, editor. J Bacteriol. 2022;204: e00036-22. doi:10.1128/jb.00036-22

Supporting Information

Fig. 1: Pulcherrimin production in liquid (top) and solid (bottom) TSS media. WT (DK1042) and isogenic mutants were grown in liquid TSS media or spotted (10 µL) onto solid TSS media and grown overnight at 37°C. The black scale marker corresponds to 5 mm.

Fig. 2: ScoC, ArbB, and PchR Control Timing and Rate of Pulcherrimin Production. A) Pulcherrimin production was measured as a function of growth phase, where T0 marks the transition from the exponential growth to stationary phase. Each panel represents the average A_{410} for a given strain compared to the A_{410} from WT (white squares). Error bars represent +/- the standard deviation. Lines running through the points are modeled using the *drm* function from the *drc* package in R (see Methods and Materials). **B)** Pulcherrimin production parameters as a function of genetic background: *i)* start of pulcherrimin production time relative to the transition phase of growth (T0), *ii)* the duration of pulcherrimin production, *iii)* the maximum estimated production rate, and *iv)* the maximum absorbance at 410 nm. For panels *i-iii,* brackets and asterisks indicate significant comparisons. For panel *iv,* brackets and "ns" indicate non-significant comparisons, where every other comparison had an adjusted p-value less than 0.05 as determined by T-test corrected for multiple comparisons with the Bonferroni correction.

Fig. 3: ScoC, PchR, and AbrB Repress the *yvmC* Promoter. A) Histograms representing fluorescence distribution as a function of cell count. In each panel, the negative control (grey, WT without GFP) was plotted with the corresponding genotype harboring a *yvmC* promoter fusion to GFP. Mean percent GFP positive with standard deviation in parentheses is provided to the right of each plot. Fluorescence was measured independently for each strain on three separate days with a representative shown**. B)** Median fluorescence for three separate trials (bar) with each trial median shown (circles). Error bars represent stand deviation between trials. Asterisks indicate an adjusted p-value less 0.05 while "ns" indicate non-significant comparisons with WT.

Fig. 4: DNAse I Protection Varies Among ScoC, PchR, and AbrB. Electropherograms of fluorescent DNAse I footprinting analysis of PchR (A), AbrB (B), and ScoC (C) with fluorescently labeled *yvmC* promoter as a function of estimated nucleotide position. Fluorescence intensity (RFU, panel *i*) of reactions incubated with (blue) and without protein (red). Differential peak height (panel *ii*) between reactions with protein and without protein. Differential peak heights less than zero indicate protection while differential peak heights greater than zero hypersensitivity.

Fig. 5: ScoC, PchR, and AbrB Bind Near the Core Promoter Region of *yvmC*. Electrophoretic mobility shift assays with WT P_{yvmC} (A) and the Δ59 promoter $P_{yvmC\Delta 59}$ (B) with increasing concentrations of purified PchR (left panel), AbrB (middle panel), and ScoC (right panel). Unshifted bands are marked with unfilled triangles, shifted bands are marked with filled triangles, and smears are marked with brackets. Proteins were diluted two-fold and final concentrations are as follows: PchR (15.6 to 250 nM for WT, 125-250

nM for Δ59), AbrB (62.5 to 1000 nM for WT, 500-1000 nM for Δ59), and ScoC (125 to 1000 nM for WT, 250-1000 nM for Δ59).

Fig. 6: Model of Pulcherrimin Regulation by ScoC, AbrB, and PchR. **A)** Pulcherriminic acid biosynthesis by the cyclization of tRNA-charged leucines to form cyclo(L-leucine-leucine) and the subsequent oxidation by CypX to form water-soluble pulcherriminic acid. Pulcherriminic acid is then transported out of the cell by YvmA, where it can form the insoluble pulcherrimin complex with iron, which forms a red color and has a peak absorbance at 410 nm. **B)** During exponential growth, PchR, AbrB, and ScoC bind directly to the *yvmC* promoter to inhibit expression of *yvmC-cypX.* Our data suggests ScoC can bind to the promoter but does so weakly. Thus, it is possible its mode of regulation may be direct or indirect through an unidentified transcriptional regulator controlled by ScoC. In any case, as nutrients become limiting, the transition state regulators become inactive, relieving repression on the *yvmC* promoter. As a MarR family transcription factor, PchR activity is likely regulated by a small ligand of which the identity is currently not known.

S1 Fig. Iron Supplementation Influences Pulcherrimin Phenotype in WT and isogenic mutants of *Bacillus subtilis.* 10 µL spots of WT and isogenic mutants on TSS (top) or LB (bottom) supplemented with different concentrations of ferric citrate. The black scale bar represents 5 mm.

S2 Fig. Cyclo-(L-leucine-L-leucine) Detection from WT and *yvmC::erm* Backgrounds. Metabolites were extracted from WT (A) and *yvmC::erm* (B) grown in liquid culture and were subject to mass spectrometry analysis for cyclo-(l-leucine-l-leucine), a precursor metabolite for pulcherrimin. The experiment was repeated at least three times with representative data shown. RT (retention time) and S/N (signal to noise ratio) for the peak corresponding to cLL are shown in each panel. The S/N ratio for *yvmC::erm* was under the limit for detection (UD, undetermined).

S3 Fig. Complementation of *scoC::erm* Restores WT Pulcherrimin Phenotype. Liquid pulcherrimin measurements from WT, *scoC::erm,* and *scoC::erm lacA::$_p$scoC-scoC* from late stationary phase cultures grown in TSS medium. Bars represent the mean A_{410} from five independent replicates.

S4 Fig. Epistasis analysis for estimated maximum production rate (mumax, right) and pulcherrimin carrying capacity (K, right). Epsilon (ε), defined as the difference between the double mutant from the log-additive effects of the corresponding single mutants (see Methods), plotted for all double and triple mutant strains. Asterisks indicate significant difference between the mean and 0 using a 1-sample t-test corrected for multiple comparisons with the Bonferroni correction.

S5 Fig. Addition of Heparin Abolishes ScoC-DNA Complexes. Similar to Fig. 5C except heparin was added to the reactions. Fluorescent DNAse I footprinting (i) and DFACE analysis with ScoC (ii). In the top panel, red electropherograms represent no protein while blue electropherograms represent reactions with protein.

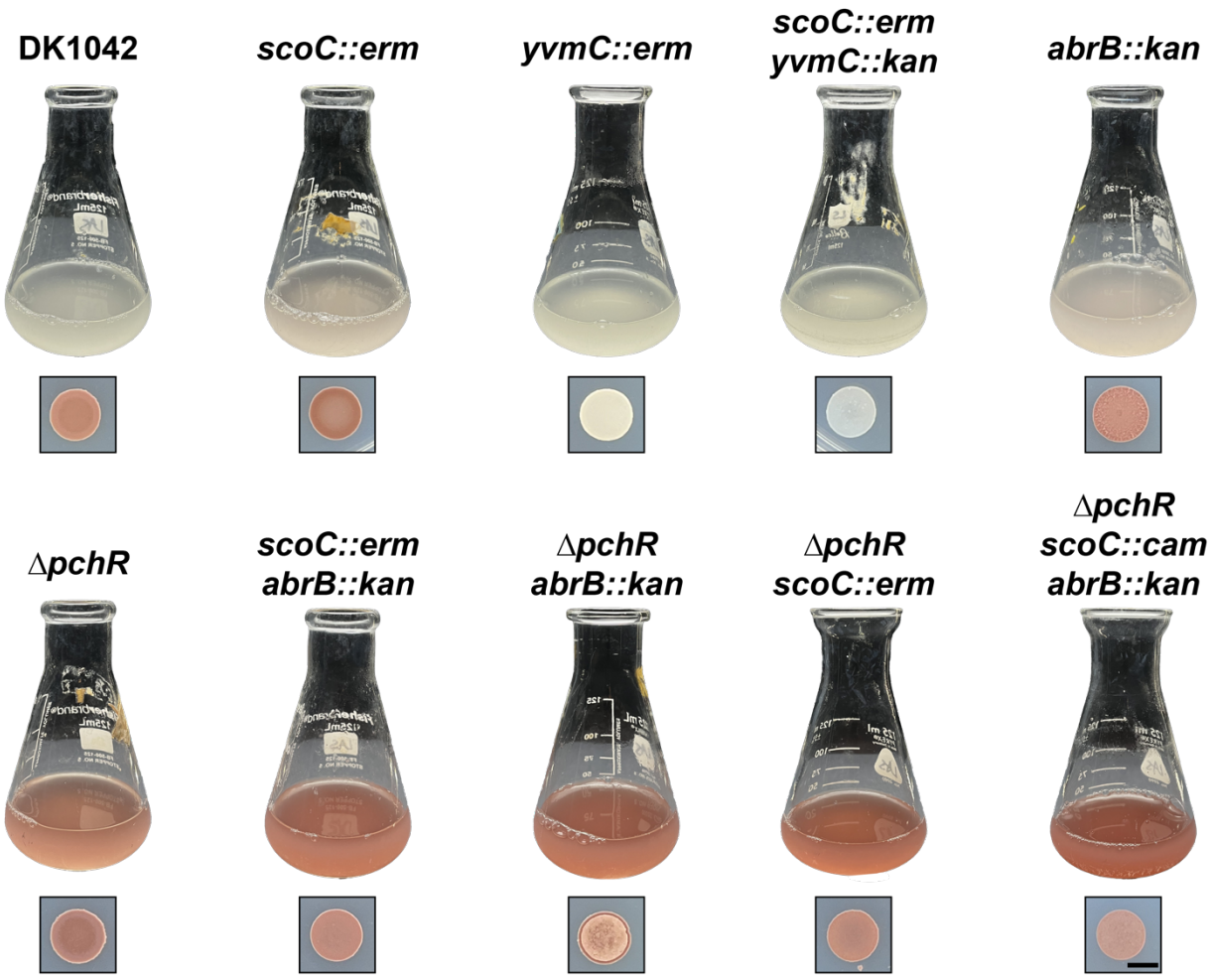

910

911 **Fig. 1: Pulcherrimin production in liquid (top) and solid (bottom) TSS media.**

912

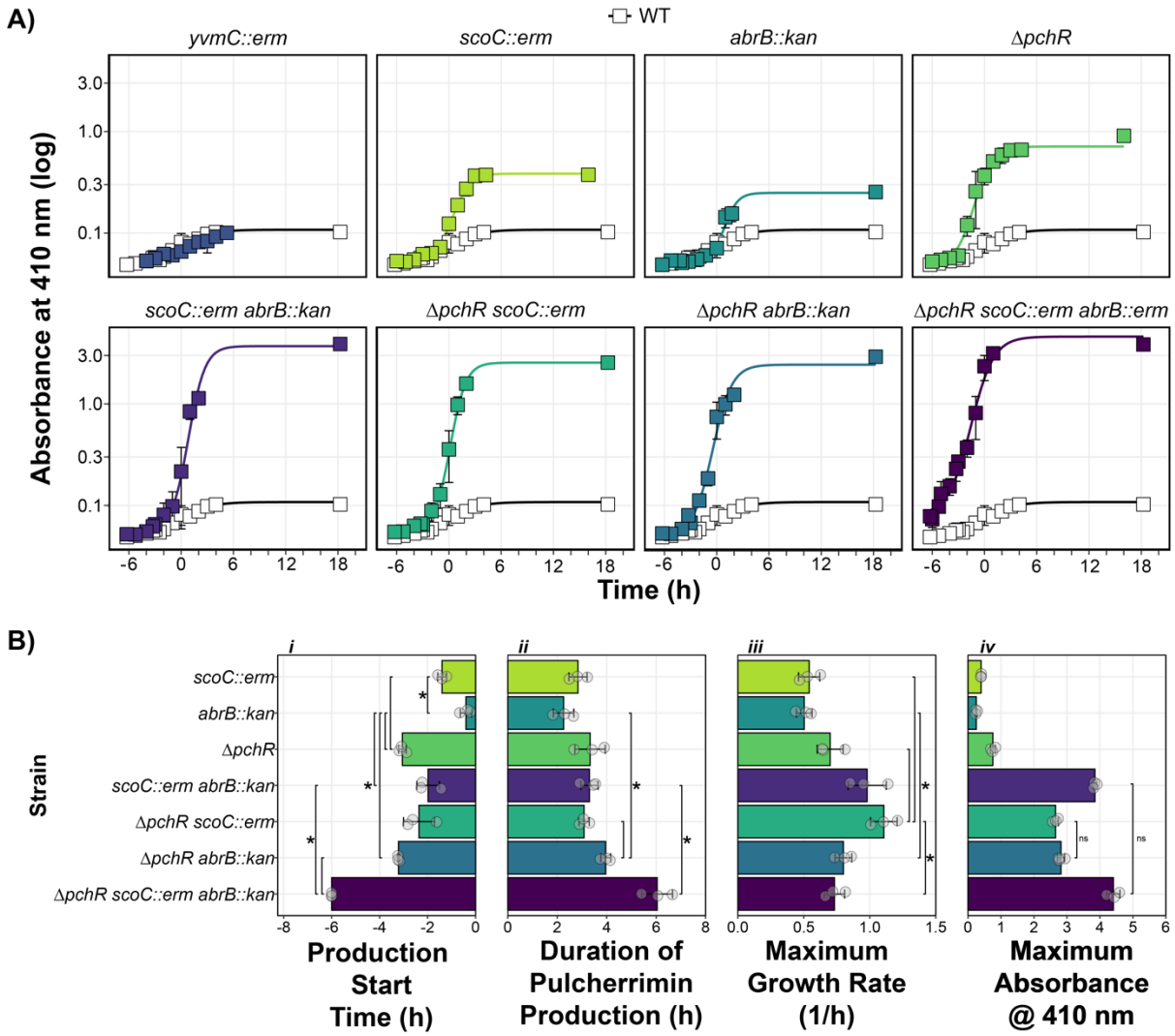

Fig. 2: ScoC, ArbB, and PchR Control Timing and Rate of Pulcherrimin Production.

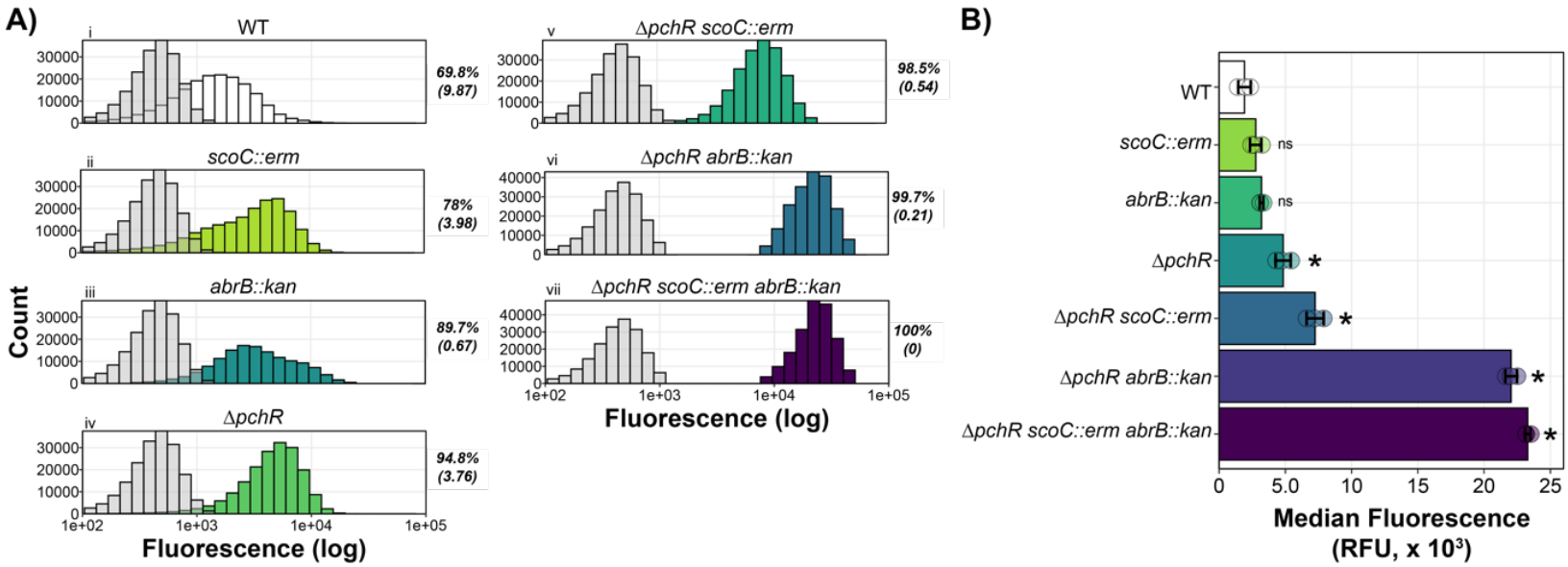

916 **Fig. 3: ScoC, PchR, and AbrB Repress the *yvmC* Promoter.**

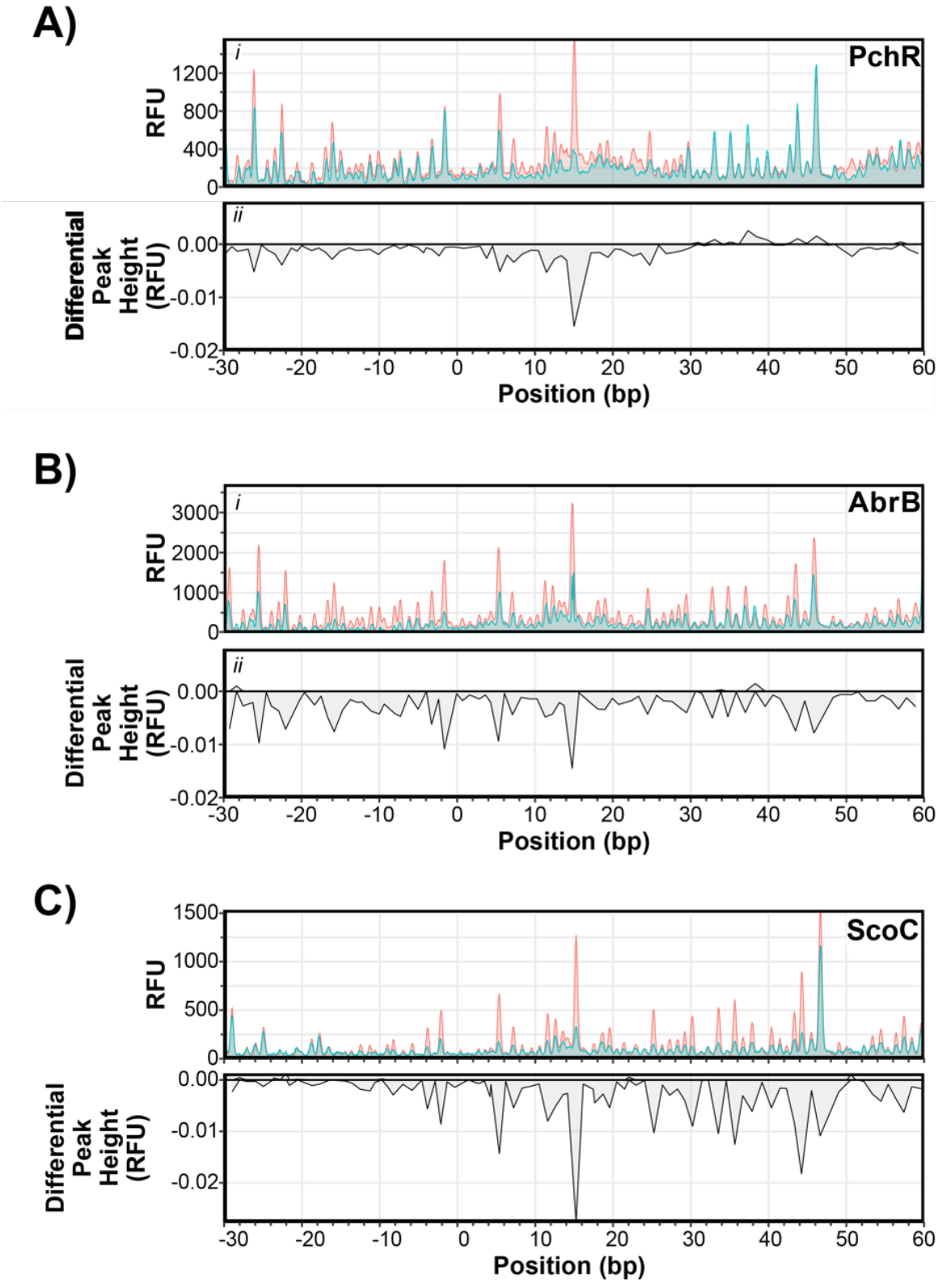

Fig 4: DNAse I Protection Varies Among ScoC, PchR, and AbrB.

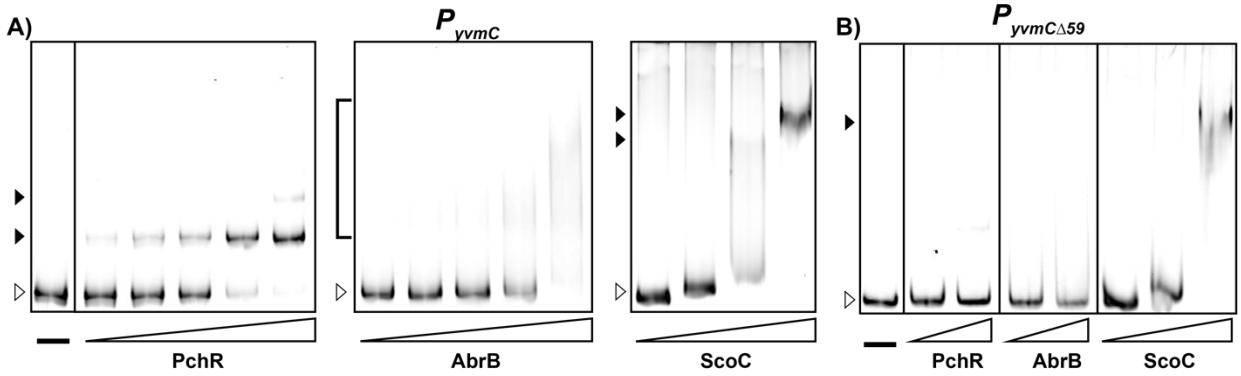

Fig. 5: ScoC, PchR, and AbrB Bind Near the Core Promoter Region of *yvmC*.

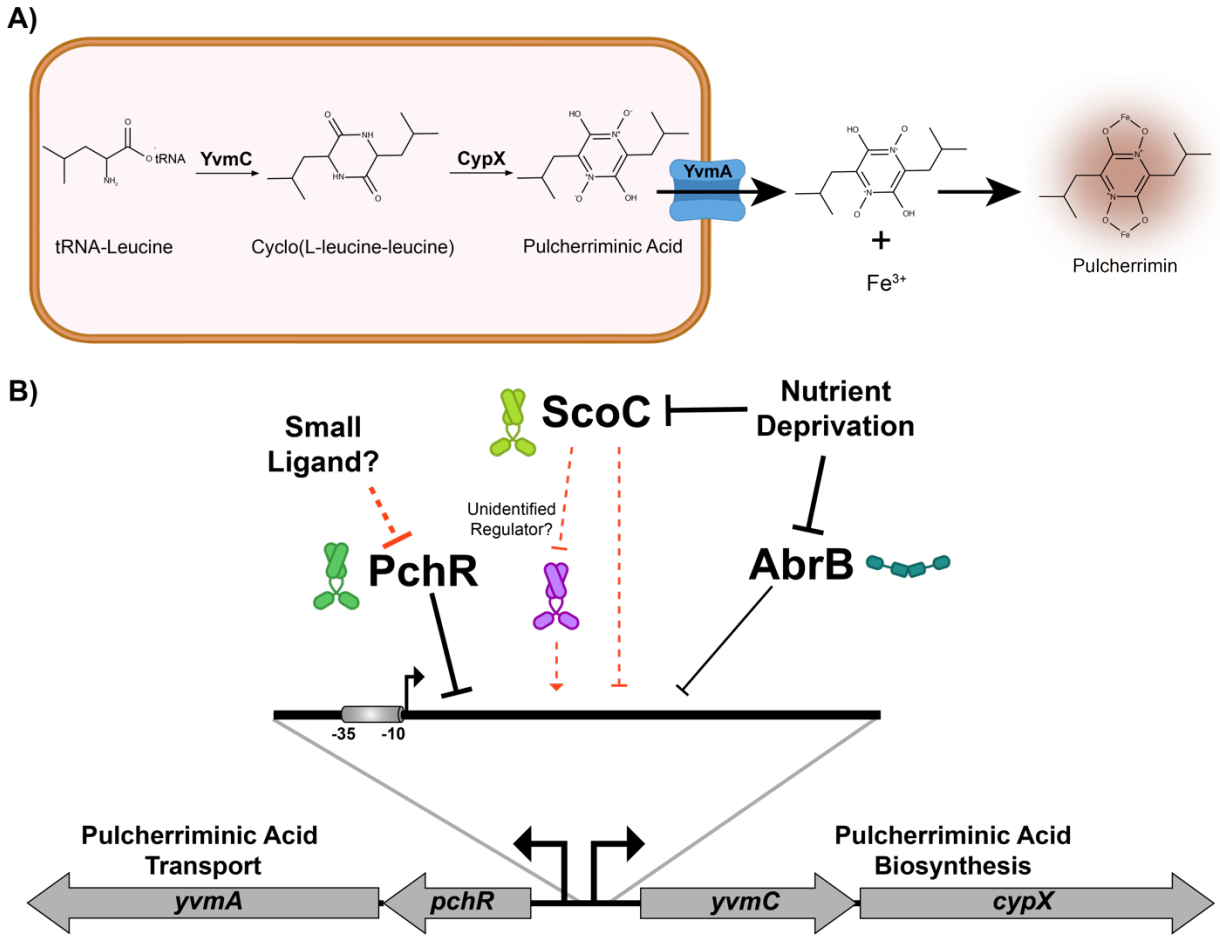

Fig. 6: Model of Pulcherrimin Regulation by ScoC, AbrB, and PchR.

941

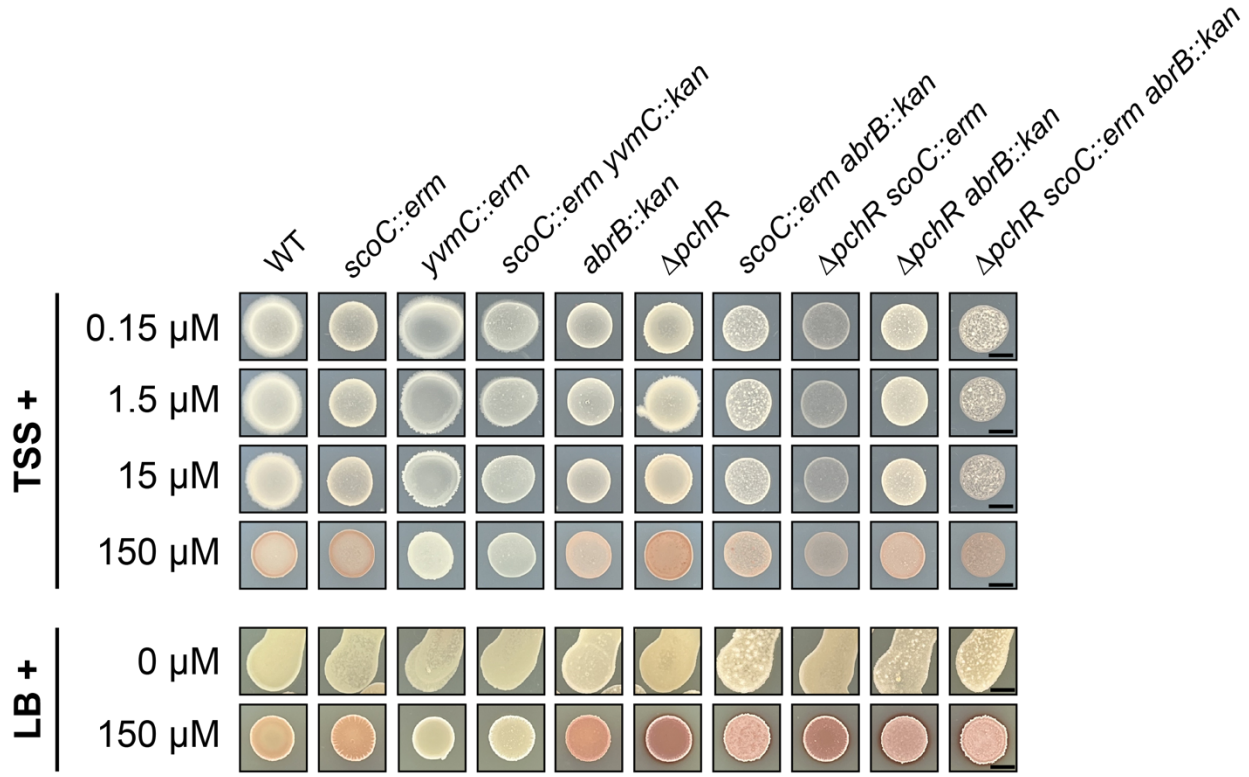

942

943 **S1 Fig.:** Iron Supplementation Influences Pulcherrimin Phenotype in WT and isogenic
944 mutants of *Bacillus subtilis.*

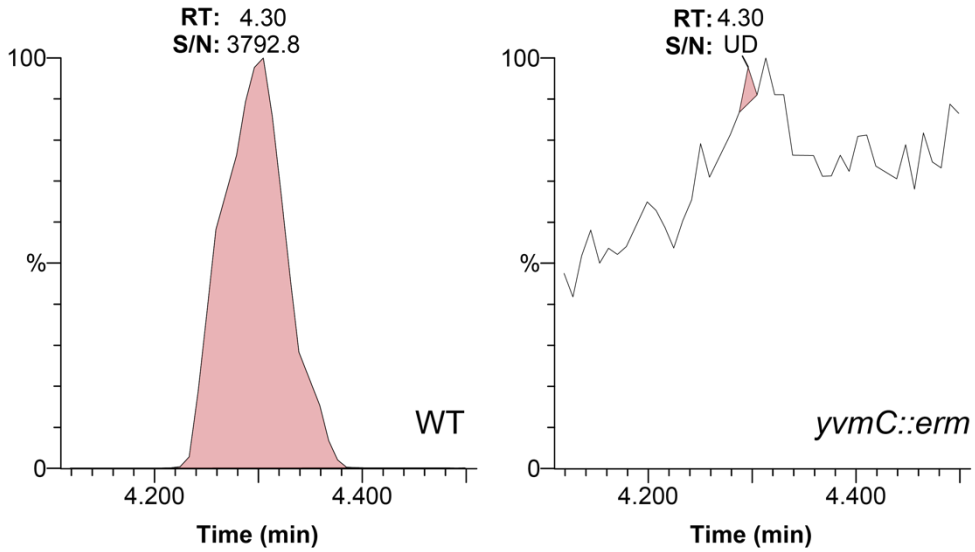

945 **S2 Fig.:** Cyclo-(L-leucine-L-leucine) Detection from WT and *yvmC::erm* Backgrounds.
946
947
948

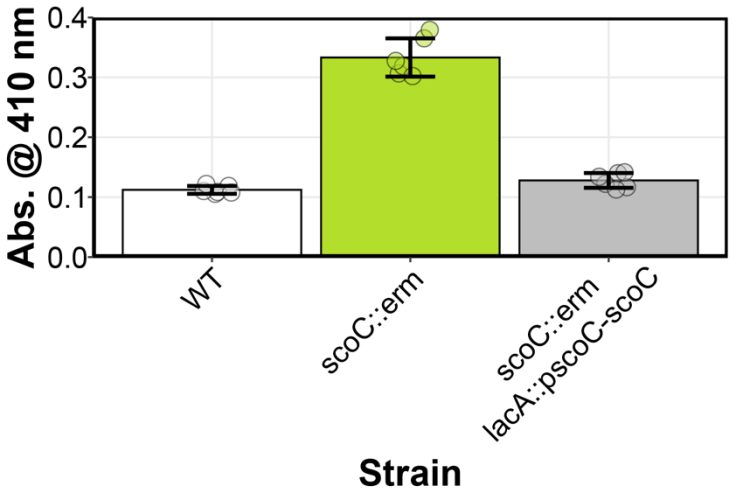

949 **S3 Fig.:** Complementation of scoC::erm Restores WT Pulcherrimin Phenotype.
950

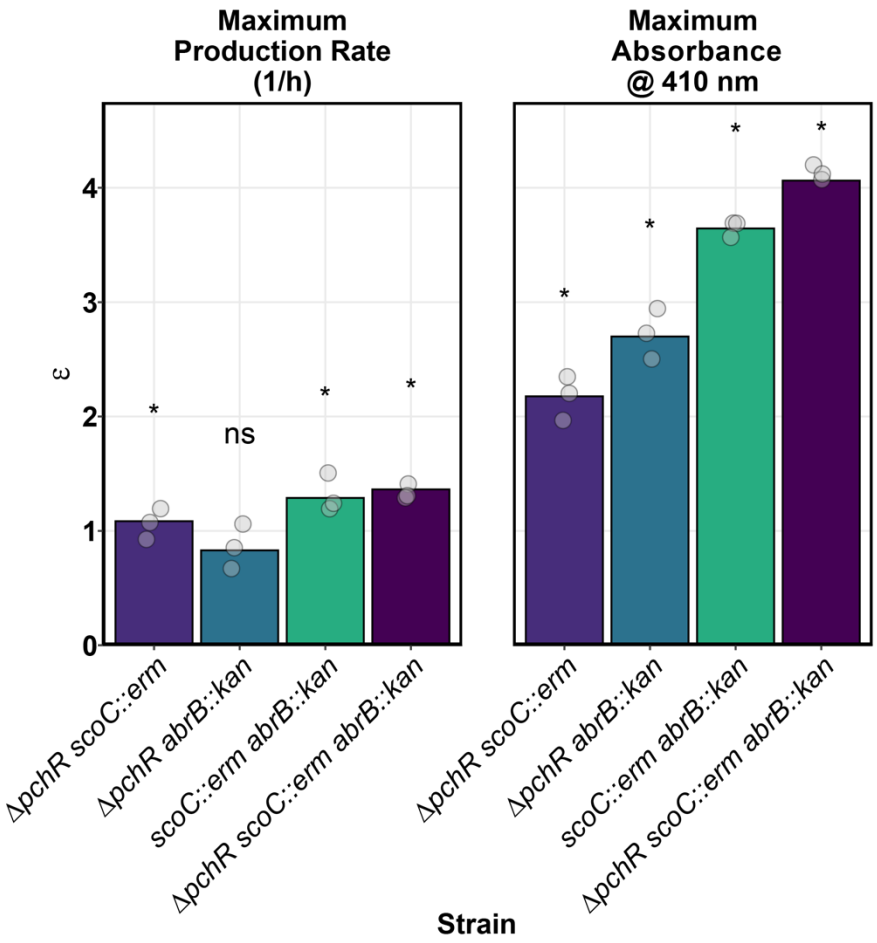

S4 Fig.: Epistasis analysis for estimated maximum production rate (mumax, right) and pulcherrimn carrying capacity (K, right).

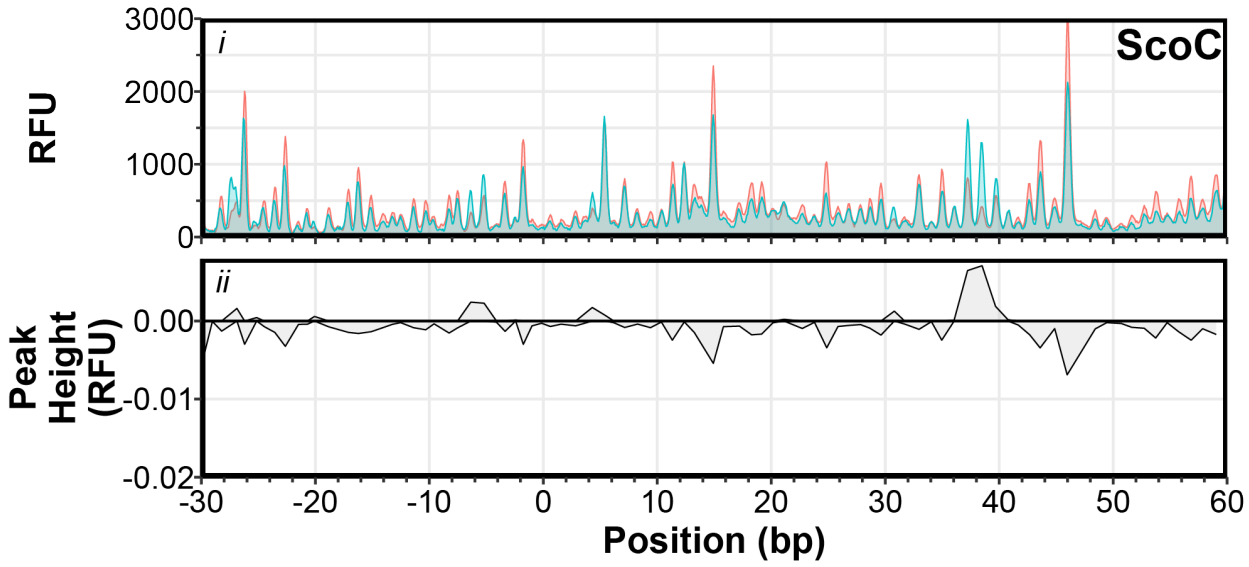

S5 Fig.: Addition of Heparin Abolishes ScoC-DNA Complexes.